Supporting Information

Pang et al. 10.1073/pnas.1303275110

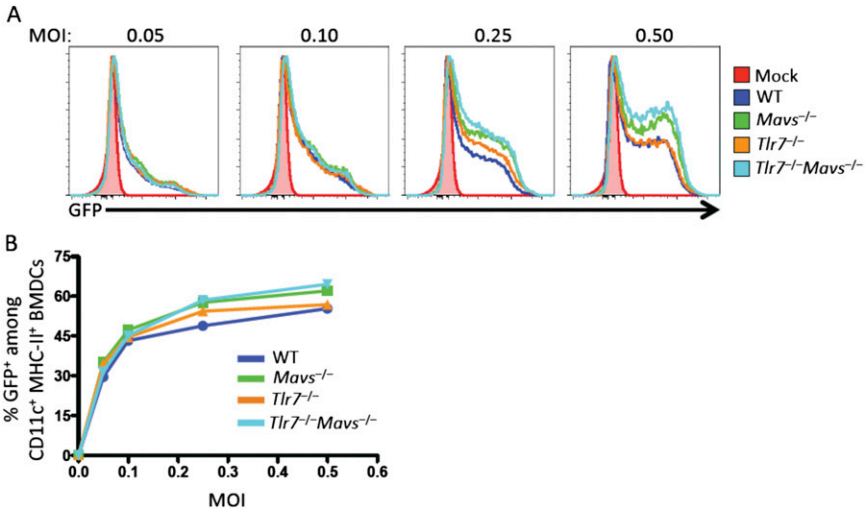

Fig. S1. The mitochondrial antiviral signaling (MAVS) and Toll-like receptor (TLR)7 signaling pathways protect against influenza virus replication in bone-marrow dendritic cells. GM-CSF cultured bone marrow-derived dendritic cells (BMDCs) from WT, *Tlr7*$^{-/-}$, *Mavs*$^{-/-}$, and *Tlr7*$^{-/-}$*Mavs*$^{-/-}$ mice were infected with PR8 NS1-GFP virus at the indicated multiplicity of infection (MOI). At 12 h postinfection, cells were harvested and stained for FACS analysis. Histograms (*A*) and frequencies (*B*) of GFP^{+} BMDCs are shown. All samples were gated on live CD11c^{+} MHC-II^{+} cells. Data represent the mean ± SEM.

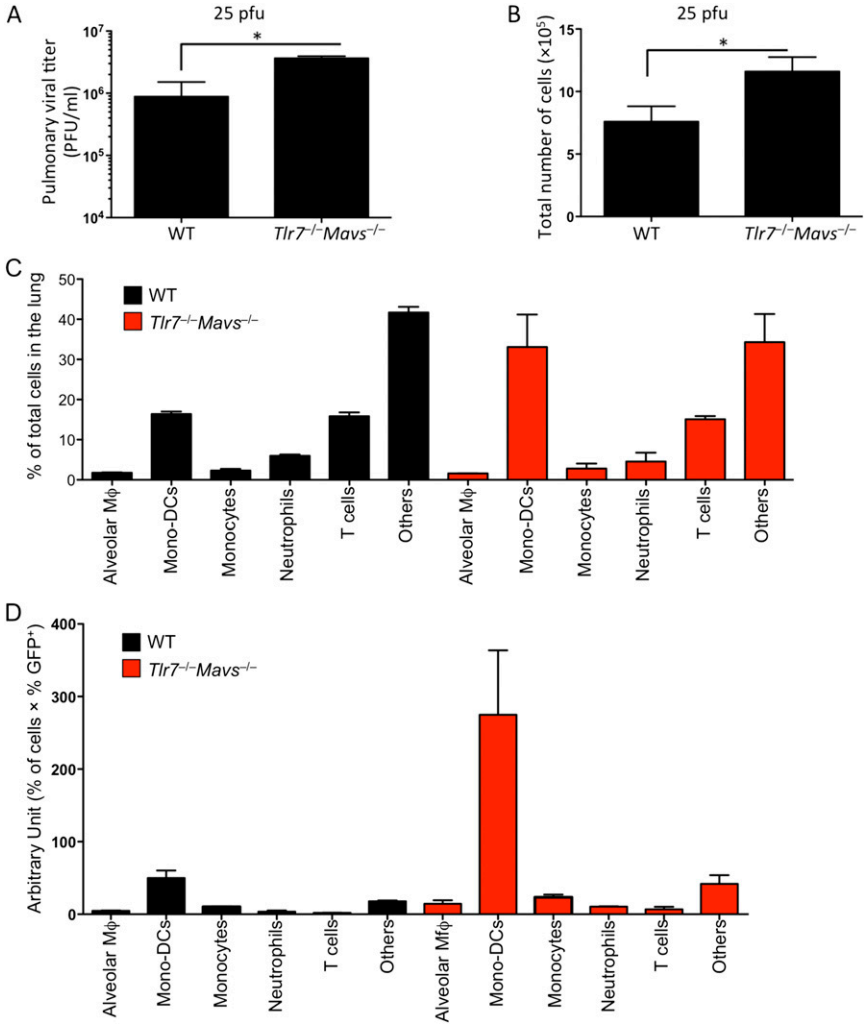

Fig. S2. TLR7 and retinoic acid inducible gene-1 (RIG-I) mediate protection against influenza virus at high viral challenge dose. WT and *Tlr7*$^{-/-}$*Mavs*$^{-/-}$ mice were infected intranasally with 25 pfu (1 LD_{50}) of A/PR8 influenza virus. At 6 d postinfection (dpi), bronchoalveolar lavage (BAL) fluids were collected from these mice and viral titers were determined by plaque assay (*A*). The total number of cells in the BAL of these mice, infected as in *A*, was enumerated at 6 dpi (*B*). (*C* and *D*) WT and *Tlr7*$^{-/-}$*Mavs*$^{-/-}$ mice were intranasally infected with 1×10^6 pfu (>300 LD_{50}) of A/PR8 NS1-GFP influenza virus. Forty-eight hours later, cells were isolated from the lung of these mice and stained for FACS analysis. The frequency (*C*) and arbitrary units of percent cell type × percent GFP^+ cells (*D*) of the indicated cell types in the lung are depicted. Data represent the mean ± SEM, $^*P < 0.05$.

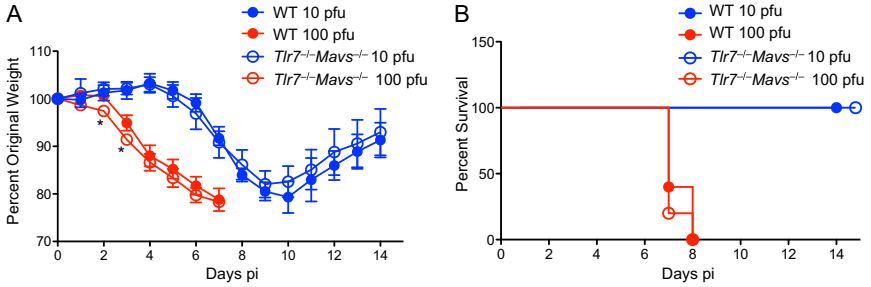

Fig. S3. Survival and weight loss of WT and *Tlr7*$^{-/-}$*Mavs*$^{-/-}$ mice after various doses of influenza viral challenge. WT (filled circles) and *Tlr7*$^{-/-}$*Mavs*$^{-/-}$ mice (open circles) were infected intranasally with 10 pfu (blue) or 100 pfu (red) of A/PR8 influenza virus. Mice were monitored daily for weight loss (*A*) and survival (*B*) following virus infection. Data represent the mean ± SEM, $^*P < 0.05$.

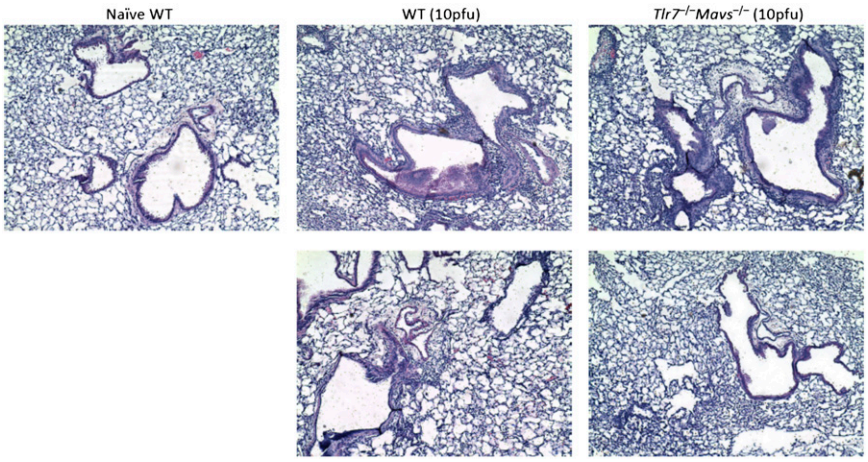

Fig. S4. Lung histopathology of influenza-infected WT and *Tlr7*$^{-/-}$*Mavs*$^{-/-}$ mice. WT and *Tlr7*$^{-/-}$*Mavs*$^{-/-}$ mice were infected intranasally with 10 pfu of A/PR8 influenza virus. At 6 dpi, the lungs were harvested, fixed in neutral buffered formalin, and paraffin-embedded for sectioning. Representative H&E-stained lung sections from naïve WT (*Left*), infected WT (*Center*), and infected *Tlr7*$^{-/-}$*Mavs*$^{-/-}$ (*Right*) mice are shown. WT and *Tlr7*$^{-/-}$*Mavs*$^{-/-}$ lungs show patchy peribronchial inflammation and bronchial infiltrates. Original magnification, 10×.

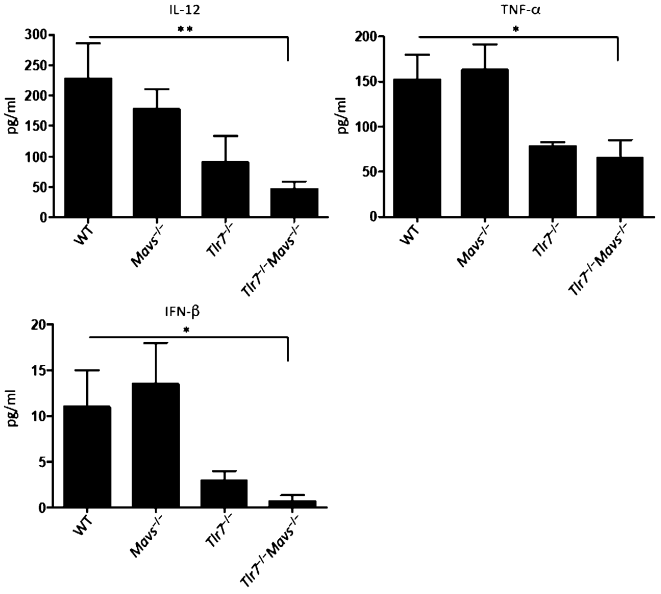

Fig. S5. Production of proinflammatory cytokines and IFN-β in the airway following influenza A virus infection. WT, *Mavs*$^{-/-}$, *Tlr7*$^{-/-}$, and *Tlr7*$^{-/-}$*Mavs*$^{-/-}$ mice were infected intranasally with 10 pfu of A/PR8 influenza virus. Lung washes were collected from these mice at 4 dpi and the levels of IL-12, TNF-α, and IFN-β were determined by ELISA. Data represent the mean ± SEM. *$P < 0.05$; **$P < 0.01$.

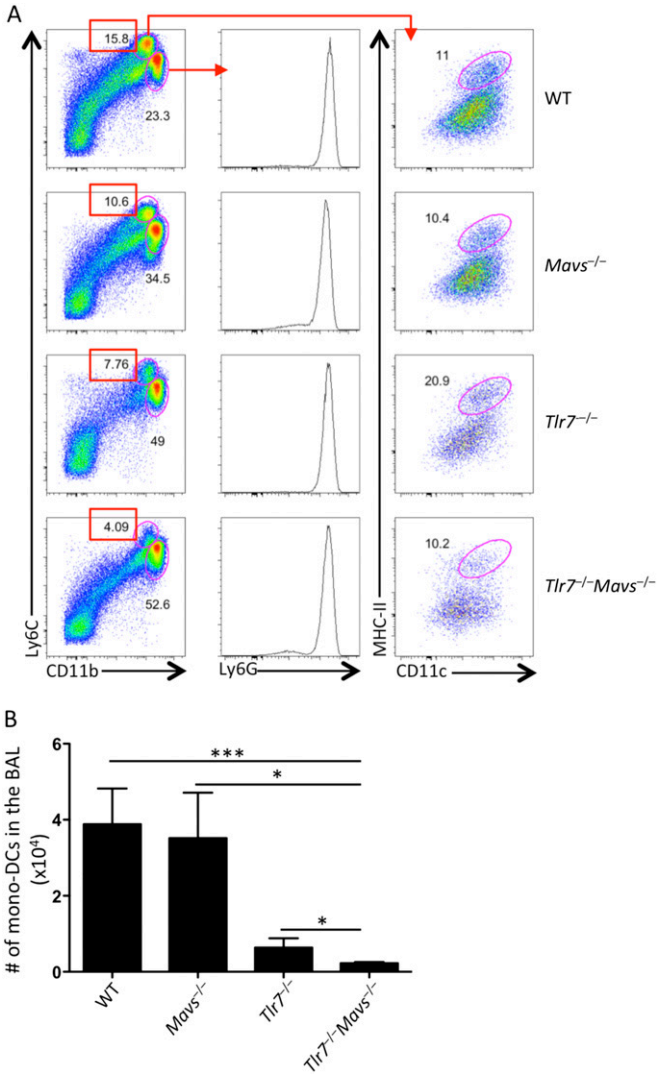

Fig. S6. The absence of TLR7 and RIG-I–mediated viral recognition lead to impaired recruitment of monocyte-derived cell populations into the airway. WT, *Mavs*$^{-/-}$, *Tlr7*$^{-/-}$, and *Tlr7*$^{-/-}$*Mavs*$^{-/-}$ mice were infected intranasally with 10 pfu of A/PR8 influenza virus. At 4 dpi, cells were harvested from the BAL fluid of these mice and stained for analysis by flow cytometry (*A*). All FACS plots were gated on live cells. Neutrophils were identified as CD11b^{+} Ly6c^{lo} Ly6G^{+} (*Center*) and monocyte-derived DCs (mono-DCs) as CD11b^{+} Ly6c^{hi} CD11c^{+} (*Right*). The numbers of mono-DCs (*B*) in the airway were enumerated. Data represent the mean ± SEM $*P < 0.05$; $***P < 0.001$.

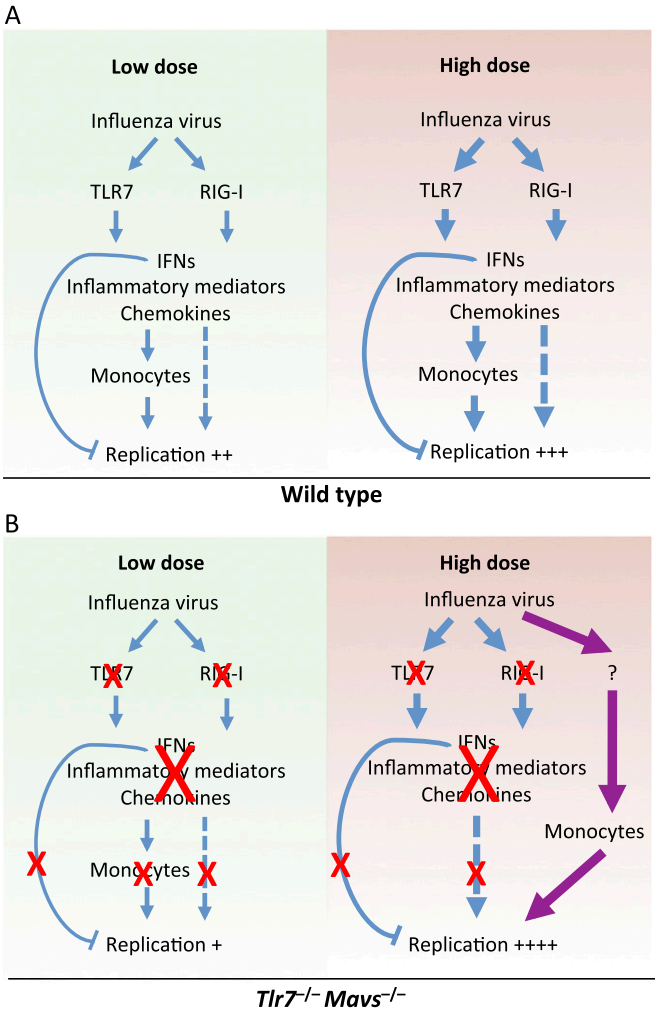

Fig. S7. Proposed model for the role of TLR7 and RIG-I pathways in virus replication during respiratory influenza A virus (IAV) infection. After a low dose of influenza infection, TLR7- and RIG-I–mediated signaling activates the induction of proinflammatory cytokines and chemokines, leading to recruitment of monocytes from the blood, which rapidly differentiate into mono-DCs in the lung. Mono-DCs are highly susceptible to IAV and serve as viral reservoirs during infection, providing a way for the virus to promote its replication in the airway (*A*, *Left*). In the absence of TLR7 and MAVS, production of inflammatory mediators and recruitment of monocytes into the lung are severely impaired, resulting in a lower viral load in the airway of *Tlr7*$^{-/-}$*Mavs*$^{-/-}$ mice (*B*, *Left*). Following a high dose of IAV challenge (*A* and *B*, *Right*), a compensatory pathway (purple arrows in *B*) in the absence of TLR7 or MAVS induces monocyte infiltration into the lung, rendering them susceptible to IAV infection in the respiratory tract of *Tlr7*$^{-/-}$*Mavs*$^{-/-}$ mice. Signals downstream of TLR7 or MAVS may also promote influenza virus replication independent of monocytes (depicted by dotted lines).